

Fluid Simulations of Intense Laser-Plasma Interactions

B. A. Shadwick, G. M. Tarkenton, E. H. Esarey and W. P. Leemans

Abstract—We present results of fluid simulations of intense laser-plasma interactions where the laser time scale is fully resolved.

Keywords—laser, plasma, numerical, fluid

THE interaction of an intense laser pulse with a plasma is a complex physical phenomenon where numerical simulation plays a key role in our still developing understanding. A wide variety of models are employed in studying these systems, ranging from full kinetic descriptions to time-averaged envelope models. Here we highlight a recently developed fluid simulation [1] which is unique in that the fast time scale of the laser pulse is explicitly resolved. This approach is less computationally intensive than a particle-in-cell simulation while retaining more of the essential physics than is present in an envelope model. In this model, the relativistic electron fluid momentum, \mathbf{p} , is driven by the Lorentz force:

$$\frac{\partial \mathbf{p}}{\partial t} + \mathbf{v} \cdot \nabla \mathbf{p} = q \left(\mathbf{E} + \frac{\mathbf{v}}{c} \times \mathbf{B} \right), \quad (1)$$

where $\mathbf{p} = \gamma m \mathbf{v}$, $\gamma = \sqrt{1 + |\mathbf{p}|^2/m^2 c^2}$, m and q are the electron mass and charge respectively, and \mathbf{E} and \mathbf{B} are the self-consistent fields obtained from Maxwell's equations with the current $\mathbf{j} = q n \mathbf{v}$, n being the fluid electron density which satisfies the continuity equation:

$$\frac{\partial n}{\partial t} + \nabla \cdot n \mathbf{v} = 0. \quad (2)$$

To keep the grid in the propagation direction of the laser to a manageable size, we transform to the usual moving-window coordinates, $(x, z, t) \mapsto (x, \xi = t - z/c, t)$. This transformation has the additional advantage of shifting all characteristic velocities by c so that *all* propagation is in the forward ξ direction which significantly simplifies the numerics.

The equations are solved on a common grid using the method-of-lines. In this method, the equations are discretized in space, yielding a large set of coupled ODEs which are then solved with a standard ODE integrator. Here we use second-order central differences in x and backwards differences in ξ . The resulting ODEs are integrated with a second order Runge–Kutta method. The Runge–Kutta algorithm was chosen because it requires less intermediate storage than other competing second-order meth-

ods. This results in a fully explicit time-advance algorithm that is manifestly charge-conserving, *i.e.*, numerically $\nabla \cdot \mathbf{E} \equiv 4\pi(n - n_{\text{ion}})$.

Fig. 1 shows results from a so-called “Standard Laser-Wakefield Accelerator” configuration wherein a short laser pulse excites a relatively large wake in an initially uniform plasma. The initial laser pulse had a Gaussian envelope in ξ centered at $\omega_p \xi = 0$ with a pulse length $\omega_p \tau = 1$, Rayleigh length $k_p Z_R = 100$, wavenumber $k_0 = 5k_p$, and dimensionless vector potential $a_0 = 1.5$. The spatial grid covered $k_p x \in [-30, 30]$ and $\omega_p \xi \in [-10, 30]$ with 601 grid points in each direction. The laser pulse was initialized in a uniform plasma and the evolution was followed until $\omega_p t = 40$ with a time step $\omega_p \Delta t = 1/60$. This run took approximately 50 min. on a 450 MHz PowerPC G4. A triangular mesh model of the surface was written to a metafile and the rendering was done with a custom application using QuickDraw3D on MacOS 9 as the underlying graphics engine. The rendering application allows for real-time manipulation of the view (orientation, lighting placement, *etc.*) as well as final rendering at high-resolution with illumination and per-pixel shading.

The plasma density, longitudinal electric field and γ are shown in Fig. 1 (a)–(c) respectively. The laser pulse is propagating to the right and is located at approximately $\omega_p \xi = 1$. Clearly the plasma wave is highly non-sinusoidal, exhibiting the characteristic shape of a non-linear wakefield, as we expect for $a_0 = 1.5$. The curvature of the phase-fronts is the result of a relativistic shift in the plasma frequency due to the transverse profile of γ , leading to a lower effective plasma frequency on axis. The noticeable increase in the plasma wave amplitude towards the back of frame [2] results from depletion of the laser pulse as it deposits energy in the plasma. The plasma wave at the left of the image was generated at an earlier time (and by a more intense laser pulse) than the plasma wave immediately behind the laser. Notice both the longitudinal component of the laser pulse as well as the density modulation at $2k_0$ inside the laser pulse are clearly visible.

In addition to the case of uniform ion density, this code can handle ion density profiles with arbitrary x and ξ variation. Using this feature, we are currently exploring laser propagation and wakefield structure in plasma channels.

REFERENCES

- B. A. Shadwick is with the Institute for Advanced Physics, 10875 U.S. Hwy. 285, Suite 199, Conifer, CO 80433 and the Center for Beam Physics, Ernest Orlando Lawrence Berkeley National Laboratory, University of California, Berkeley, CA 94720.
 G. M. Tarkenton is with the Institute for Advanced Physics.
 E. H. Esarey and W. P. Leemans are with the Center for Beam Physics.
- [1] B. A. Shadwick, G. M. Tarkenton, E. H. Esarey, and W. P. Leemans, “Fluid Modeling of Intense Laser-Plasma Interactions,” in *Advanced Accelerator Concepts, Ninth Workshop*, Santa Fe, NM, No. 569 in *AIP Conference Proceedings*, edited by P. L. Colestock and S. Kelly (AIP, Melville, NY, 2001), pp. 154–162.
 - [2] B. A. Shadwick, G. M. Tarkenton, E. H. Esarey, and W. P. Lee-

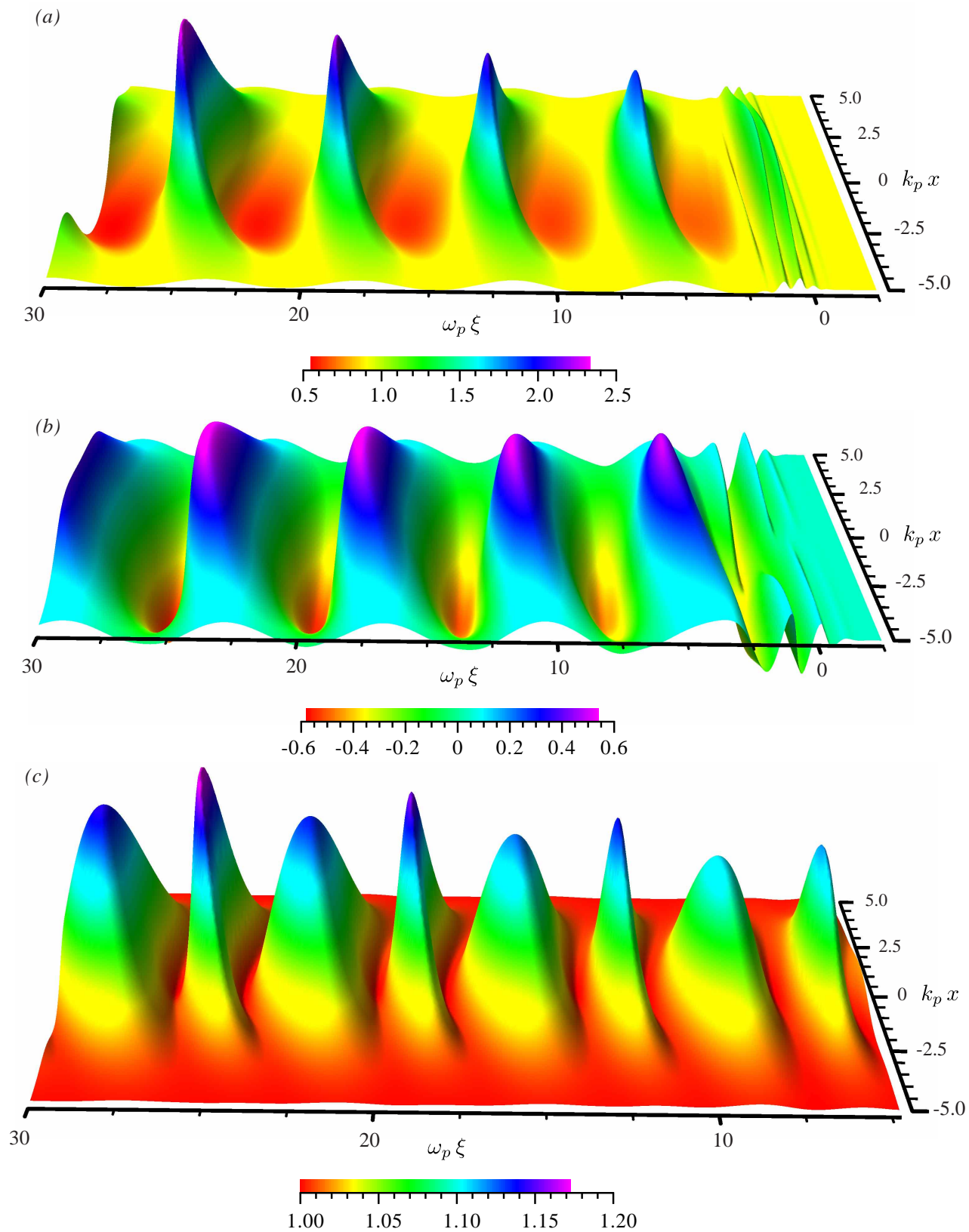


Fig. 1. Plasma response at $\omega_p t = 40$ to a high-intensity short laser pulse: (a) electron density; (b) longitudinal electric field in units of the cold wave-breaking field $m c \omega_p / q$ and (c) relativistic factor γ (shown only behind the laser). The laser is propagating to the right.